Helicobacter pylori Adaptation In Vivo in Response to a High-Salt Diet

John T. Loh,[a] Jennifer A. Gaddy,[a,c] Holly M. Scott Algood,[a,b,c] Silvana Gaudieri,[a,d,e] Simon Mallal,[a,b,e] 🆔 Timothy L. Cover[a,b,c]

Department of Medicine,[a] Department of Pathology, Microbiology and Immunology,[b] Vanderbilt University School of Medicine, and Veterans Affairs Tennessee Valley Healthcare System,[c] Nashville, Tennessee, USA; School of Anatomy, Physiology, and Human Biology, University of Western Australia, Nedlands, Western Australia, Australia[d]; Institute for Immunology and Infectious Diseases, Murdoch University, Murdoch, Western Australia, Australia[e]

Helicobacter pylori exhibits a high level of intraspecies genetic diversity. In this study, we investigated whether the diversification of H. pylori is influenced by the composition of the diet. Specifically, we investigated the effect of a high-salt diet (a known risk factor for gastric adenocarcinoma) on H. pylori diversification within a host. We analyzed H. pylori strains isolated from Mongolian gerbils fed either a high-salt diet or a regular diet for 4 months by proteomic and whole-genome sequencing methods. Compared to the input strain and output strains from animals fed a regular diet, the output strains from animals fed a high-salt diet produced higher levels of proteins involved in iron acquisition and oxidative-stress resistance. Several of these changes were attributable to a nonsynonymous mutation in fur (fur-R88H). Further experiments indicated that this mutation conferred increased resistance to high-salt conditions and oxidative stress. We propose a model in which a high-salt diet leads to high levels of gastric inflammation and associated oxidative stress in H. pylori-infected animals and that these conditions, along with the high intraluminal concentrations of sodium chloride, lead to selection of H. pylori strains that are most fit for growth in this environment.

*H*elicobacter pylori is a Gram-negative bacterium that persistently colonizes the human stomach in half of the world's population (1, 2). *H. pylori* exhibits a high level of intraspecies genetic diversity, characterized by marked variation among strains in gene content, as well as a high level of variation in the nucleotide sequences of individual genes (3, 4). A high rate of allelic diversity is attributable to both a high mutation rate and intraspecies recombination (5, 6).

Most *H. pylori*-infected persons remain asymptomatic, but the presence of this bacterium increases the risk of peptic ulcer disease and gastric cancer (1, 2, 7, 8). The clinical outcome of *H. pylori* infection is determined by a combination of bacterial, host, and environmental factors. For example, *H. pylori* strains containing the *cag* pathogenicity island (PAI) are associated with a higher risk of symptomatic disease than are strains that lack the *cag* PAI (9). One of the proteins encoded by the *cag* PAI, CagA, enters host cells and causes numerous cellular alterations linked to malignant transformation (10). The *cag* PAI also encodes multiple protein components of a type IV secretion system required for entry of CagA into host cells (11). *H. pylori* strains that secrete specific types of the VacA toxin are also linked to adverse disease outcome, in comparison to strains that secrete relatively nontoxic forms of the VacA protein (12, 13).

One of the environmental factors associated with increased gastric cancer risk is a high-salt diet (14). Epidemiologic studies have demonstrated a link between high dietary salt consumption and increased gastric cancer risk in many parts of the world (15–17), and a high-salt diet also increases the gastric cancer risk in animal models (18–21). For instance, in *H. pylori*-infected Mongolian gerbils treated with a chemical carcinogen, high dietary salt consumption was associated with an increased incidence of gastric cancer (21). Another study reported that *H. pylori* infection and a high-salt diet could independently induce atrophic gastritis and intestinal metaplasia in Mongolian gerbils (18). More recently, administration of a high-salt diet to Mongolian gerbils infected

with an *H. pylori* strain harboring a functionally active *cag* PAI-encoded type IV secretion system was shown to increase the incidence of gastric cancer, compared to what was observed in infected animals fed a regular diet (22). Infected animals fed a high-salt diet had more severe gastric inflammation, a higher gastric pH, greater parietal cell loss, greater gastric expression of interleukin-1β, and lower gastric expression of hepcidin and hydrogen potassium ATPase than those on a regular diet (22). Several studies have demonstrated that *H. pylori* responds *in vitro* to alterations in the sodium chloride concentration of the culture medium. Salt-responsive changes include alterations in bacterial morphology, altered expression of specific *H. pylori* genes, and altered abundance of specific *H. pylori* proteins (23–26). Increased production of CagA in response to high-salt conditions may be one factor that accounts for the increased risk of gastric cancer associated with a high-salt diet (22, 24, 25).

In the present study, we tested the hypothesis that prolonged exposure of *H. pylori in vivo* to the gastric environmental conditions associated with a high-salt diet might lead to the emergence of strains adapted to these conditions. We show that the production of proteins involved in iron acquisition and oxidative-stress

B128 (isolated from a human stomach)

infect Mongolian gerbil

7.13 (isolated from Mongolian gerbil)

Gerbils fed a regular salt diet
(n=19)

Regular salt output (RSO) strains
(n=9)

Proteomics on strains from
2 gerbils (RSO241, RSO242)

Genome sequencing of
RSO 241 (4 single colonies)

Proteomics and
genome sequencing
of input strain
(4 single colonies)

Gerbils fed a high salt diet
(n=19)

High salt output (HSO) strains
(n=9)

Proteomics on strains from
2 gerbils (HSO1, HSO123)

Genome sequencing of
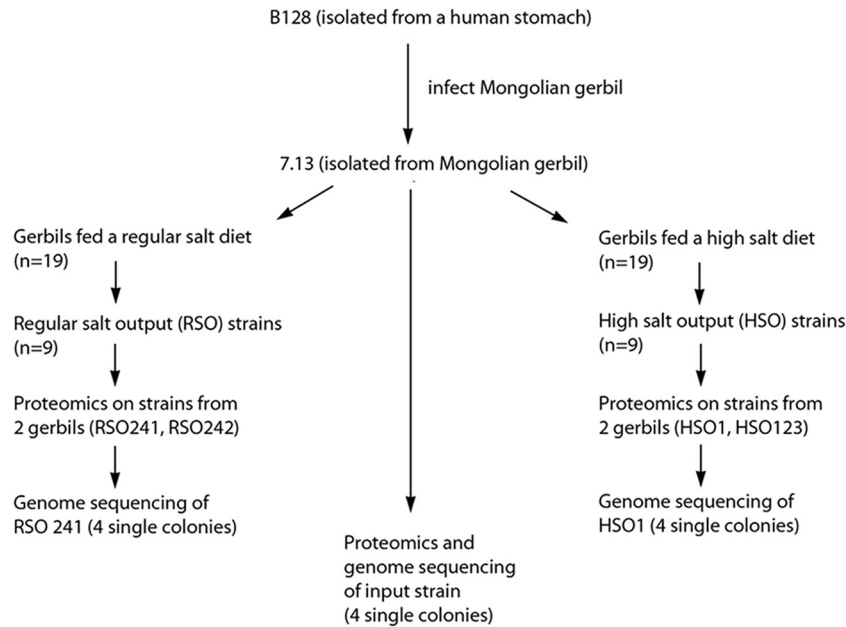HSO1 (4 single colonies)

FIG 1 Schematic illustrating genomic and proteomic analyses of *H. pylori* strains. Gerbils were infected with *H. pylori* strain 7.13, and the animals were fed either a regular or a high-salt diet. Output strains from nine gerbils fed a regular diet (RSO) and nine gerbils fed a high-salt diet (HSO) were subsequently analyzed. Strains from two gerbils on a regular diet (RSO241 and RSO242) and two gerbils on a high-salt diet (HSO1 and HSO123) and input 7.13 strain were analyzed by a proteomics approach. Strains RSO241 and HSO1 and the input strain (four single colonies of each) were analyzed by whole-genome sequencing.

resistance in *H. pylori* strains cultured from animals on a high-salt diet differs from that of the input strain and strains isolated from animals on a regular diet. We show that a nonsynonymous mutation in *fur* (encoding the Fur transcriptional regulator) accounts for the altered production of several of the differentially abundant proteins, and we show that strains harboring this *fur* mutation exhibit increased resistance to high-salt conditions and oxidative stress *in vitro*. These results reveal that the evolution of *H. pylori* within a host can be shaped by the composition of the diet. Since consumption of a high-salt diet in a setting of *H. pylori* infection results in gastric environmental conditions that are markedly different from those associated with a regular-salt diet (22), we propose that there is strong positive selection for *H. pylori* strains that are most fit for growth in the high-salt gastric environment.

MATERIALS AND METHODS

Bacterial strains and culture methods. *H. pylori* strain B128 was originally isolated from the stomach of a human with gastric ulcer disease and was subsequently used for orogastric infection of Mongolian gerbils (27, 28). The strain isolated from one of these gerbils (B128 7.13) was designated strain 7.13 in a previous study (27) (Fig. 1). We recently conducted a study in which we infected a cohort of gerbils with strain 7.13 and fed the infected animals either a regular Purina 5001 (Purina, LLC) diet (0.75% NaCl) or a Purina 5001 high-salt diet (8.75% NaCl) (22). At 16 weeks postinfection, the animals were euthanized and their stomachs were excised (22). Strains were recovered from each of the animals by plating homogenized stomach tissue onto selective medium (22). Bacteria from a single plate (containing multiple colonies) were gathered into 0.5 ml of brucella broth, and 0.5 ml of 60% glycerol was added to create a freezer stock. In the present study, we analyzed strains that were cultured from these animals (output strains). Specifically, we analyzed strains cultured from nine animals on a regular diet (regular-salt output [RSO] strains) and nine animals on a high-salt diet (high-salt output [HSO] strains) (Fig. 1). Freezer stocks of the isolated *H. pylori* output strains were recovered by

plating onto Trypticase soy agar plates containing 5% sheep blood (Hemostat Laboratories), vancomycin (20 μg/ml; Sigma-Aldrich), nalidixic acid (10 μg/ml; Sigma-Aldrich), bacitracin (30 μg/ml; Sigma-Aldrich), and amphotericin B (2 μg/ml; Sigma-Aldrich) to select for *H. pylori* growth. These plates were incubated at 37°C in a microaerobic chamber (BD GasPak EZ Campy container system) for 5 days. Subsequently, *H. pylori* strains were grown on Trypticase soy agar plates supplemented with sheep blood, in modified brucella broth containing 5% fetal bovine serum (BB-FBS), or on BB-FBS agar plates in room air supplemented with 5% CO_2 at 37°C. When necessary, BB-FBS agar plates were supplemented with streptomycin (25 μg/ml) or chloramphenicol (5 μg/ml). *Escherichia coli* strains were grown on Luria-Bertani medium. When necessary, the *E. coli* culture medium was supplemented with ampicillin (50 μg/ml), chloramphenicol (25 μg/ml), or streptomycin (25 μg/ml).

Proteomic analyses. Two independent proteomic experiments were performed. Experiment 1 compared the proteome of strain 7.13, which was used previously for infection of gerbils (22) (input strain), with that of output strains RSO242 and HSO123, and experiment 2 compared the proteome of the input strain with that of output strains RSO241 and HSO1. *H. pylori* strains were grown overnight in BB-FBS to an optical density at 600 nm (OD_{600}) of about 0.5 and then subcultured (1:10) into fresh BB-FBS for 15 h (OD_{600} of about 0.5). Bacterial cultures were harvested by centrifugation at 3,500 × *g*, and the pellets were resuspended in phosphate-buffered saline. Following a second centrifugation at 3,500 × *g*, pellets were resuspended in Tris buffer containing cOmplete protease inhibitor cocktail (Roche) as described previously (29). Bacteria were lysed by sonication, and lysates were clarified by centrifugation. These preparations were then analyzed by multidimensional protein identification technology (MudPIT) as described previously (29–31). Peptide tandem mass spectra were queried with SEQUEST (full tryptic specificity) against an *H. pylori* strain B8 (a closely related strain for which a complete genome sequence is available) (32) database to which both common contaminants and reversed versions of the proteins had been appended. B8 is the designation given previously to a strain that was cultured from Mongolian gerbils infected with *H. pylori* strain B128 (32). Since strains 7.13

and B8 each originated from the same parent strain (human isolate B128) and each was generated by experimentally infecting gerbils with strain B128, these lineages are predicted to be very closely related. Resulting identifications were filtered to an estimated peptide false-discovery rate of <5% and collated by protein with IDPicker 3.0. All subsequent analyses were performed in Excel. All reported proteins were identified on the basis of the detection of a minimum of two distinct peptides. For the complete proteomic data, see Table S1 in the supplemental material.

H. pylori genome sequence analysis. DNA samples were prepared from *H. pylori* cells with the Wizard genomic purification kit (Promega). DNA samples were nebulized, and products from each sample were combined with multiplex identifier adaptors during library construction prior to pooling (two samples per lane) and then clonally amplified on capture beads in water-in-oil emulsion microreactors. Next-generation sequencing of the libraries was accomplished with the 454 Life Sciences platform (GS-FLX; Roche Applied Science, Penzburg, Germany). The average level of coverage for the sequenced strains was 18-fold (ranging from 13- to 26-fold). Nucleotide data were collected and analyzed with Genome Sequencer software (Roche Applied Science) and in-house programs to evaluate the quality of sequence reads and to identify likely homopolymer errors. All sequence reads were aligned with the genome sequence of *H. pylori* strain B8 (GenBank accession no. NC_014256.1), a closely related strain whose complete genome sequence is available [32]. As described above, strains 7.13 and B8 each originated from the same parent strain (human isolate B128) and each was generated by experimentally infecting gerbils with strain B128. Therefore, these lineages are predicted to be very closely related.

Real-time PCR. Overnight broth cultures of *H. pylori* output strains were subcultured into fresh brucella broth and grown for 5 h (OD_{600} of ~0.5 to 0.6). Total RNA was isolated from *H. pylori* with TRIzol reagent (Gibco). RNA samples were digested with RQ1 RNase-free DNase (Promega) to remove contaminating DNA, and the RNA samples were then subjected to a cleanup step with RNeasy columns (Qiagen). cDNA synthesis was performed with 100 ng of purified RNA with the first-strand iScript cDNA synthesis kit (Bio-Rad). As controls, first-strand cDNA synthesis reactions without reverse transcriptase were carried out in parallel. The cDNA and control preparations were diluted 1:20 and used in real-time PCRs. Real-time PCR was performed with an ABI Real Time PCR machine (Step One Plus) with SYBR green as the fluorochrome. Transcript abundance was assessed by the $\Delta\Delta C_T$ method (C_T, cycle threshold), with each transcript signal normalized to the abundance of the 16S rRNA internal control. The normalized transcript signal for each biological sample was then divided by similarly normalized values from control samples to obtain a relative expression ratio. The primers used for real-time analysis were as follows: 16S rRNA, 5′-GGAGTACGGTCGCAAGATTAAA-3′ and 5′-CTAGCGGATTCTCTCAATGTCAA-3′; *katA*, 5′-TCCACTTTGAAACCATGCAA-3′ and 5′-TACAATGCCCACTTCCATCA-3′; *frpB1*, 5′-GAAATTCTTTTGGCGATCCA-3′ and 5′-TCCTAGGCTGTGAGCTTGGT-3′; *fecA1*, 5′-ATGGTATGCGAACTACCGCC-3′ and 5′-TAGCGTTGCCCCACTTCAAT-3′; *pdxA*, 5′-CTCAAAGCGGGGCGTATAGT-3′ and 5′-GGTATGCCCCACAAAAGGGA-3′; *gyrB*, 5′-CGTGGATAACGCTGTAGATGAGAGC-3′ and 5′-GGGATTTTTTCCGTGGGGTG-3′.

Analysis of catalase enzymatic activity. To measure catalase activity, overnight broth cultures of *H. pylori* were inoculated into fresh brucella broth and grown to an OD_{600} of ~0.5 to 0.6. After the samples were normalized to an OD_{600} of 0.1, catalase enzymatic assays were performed with the Amplex red catalase kit (Life Technologies). The catalase activity in 2-fold serial dilutions of culture samples was compared to the catalase activity associated with the purified catalase standards provided in the Amplex red catalase kit (Life Technologies). Enzymatic measurements were performed in accordance with the manufacturer's instructions.

Mutagenesis of Fur. To introduce unmarked mutations into the *fur* gene of *H. pylori* strain 7.13 (input strain) or output strain RSO251, a counterselection method using a *cat-rpsL* cassette was employed [33, 34].

As a first step in counterselection mutagenesis, *H. pylori rpsL* mutants were generated by transformation of *H. pylori* with a plasmid containing a cloned *H. pylori rpsL* gene harboring an A-to-G mutation at codon 43 of *rpsL* [34]. This mutation results in a Lys (K)-to-Arg (R) amino acid substitution at position 43, and *H. pylori* strains bearing this mutation are streptomycin resistant. The Sm^r *rpsL*-K43R mutants were then transformed with p*fur::cat-rpsL*, a nonreplicating plasmid that allows the insertion of a *cat-rpsL* cassette into the *fur* open reading frame (ORF). This cassette confers resistance to chloramphenicol mediated by the chloramphenicol acetyltransferase (*cat*) gene from *Campylobacter coli* and susceptibility to streptomycin mediated by the intact *rpsL* gene from *H. pylori* 26695. To generate the p*fur::cat-rpsL* plasmid, primers 5′-TTACCCGCATGATTATAACGGCTA-3′ and 5′-GCGATAAAGGCGTGGTGTT-3′ were utilized to PCR amplify a DNA product from *H. pylori* 7.13 genomic DNA extending from approximately 300 bp upstream of the *fur* translational start site to 900 bp downstream of the *fur* translational start site. This PCR product was cloned into pGEM-T Easy (Promega), and the resultant *fur*-containing plasmid was used as a template for inverse PCR with primers 5′-CGACCGCTTTTTGAAGTCTC-3′ and 5′-CGCTATGAAATTGCGGCTAAAG-3′ to facilitate the insertion of the *cat-rpsL* cassette [33]. After ligation with the *cat-rpsL* cassette, the resultant plasmid (p*fur::cat-rpsL*), which is unable to replicate in *H. pylori*, was transformed into the *rpsL*-K43R mutants of *H. pylori* strains 7.13 and RSO251, and single colonies resistant to chloramphenicol (5 μg/ml) but sensitive to streptomycin (25 μg/ml) were selected. Introduction of the *cat-rpsL* cassette into the *fur* genes of strains 7.13 and RSO251 was confirmed by PCR amplification and DNA sequencing.

A *fur*-containing plasmid was used as the template for targeted mutagenesis with the Quik-Change mutagenesis kit (Agilent Technologies). The introduction of mutations within the codon encoding Fur amino acid 88 was confirmed by DNA sequencing. These mutated plasmids were then used to transform *H. pylori* strains harboring *fur::cat-rpsL*. Transformations were plated onto BB-FBS agar plates containing streptomycin (25 μg/ml), and streptomycin-resistant colonies were isolated. DNA sequencing was used to confirm the loss of the *cat-rpsL* cassette and the introduction of the desired mutations into the *fur* ORF.

Growth of H. pylori fur mutants under oxidative-stress or high-salt conditions. *H. pylori* strains harboring wild-type (WT) *fur* or *fur-R88H* were first tagged by the introduction of either a *cat* or an *aph3* cassette into the *ureA* locus of *H. pylori*. This was carried out with plasmids pAD-C and pAD-K, which contain *cat* and *aph3* cassettes, respectively, flanked by *H. pylori ureA* sequences [35]. Proper introduction of the cassettes into the *ureA* locus was confirmed by PCR analysis and DNA sequencing. We have shown previously that insertion of antibiotic cassettes into this locus does not interfere with *H. pylori* growth [31]. To test the susceptibility of *H. pylori* to oxidative-stress conditions, strains (each at 2.5×10^7 cells/ml) containing the WT *fur* or *fur-R88H* allele and expressing different antibiotic markers were coinoculated into brucella broth supplemented with 5 or 10 μM paraquat (Sigma-Aldrich) as an inducer of oxidative stress [36] or brucella broth without added paraquat. Following overnight growth to an OD_{600} of ~0.5, serial dilutions of the mixed cultures were plated on BB-FBS plates containing either chloramphenicol or kanamycin. Viable colonies were counted following 5 days of plate growth to determine the proportion of the mixed culture that harbored either the WT *fur* or the *fur-R88H* allele. A similar experimental design was used to compare the sensitivities of the WT and *fur-R88H* mutant strains to high-salt conditions with brucella broth supplemented with 1.2% NaCl.

Statistical methods. The statistical significance of differences was analyzed by either Mann-Whitney test (for nonparametric data) or *t* test with GraphPad Prism 5 software (GraphPad Software, La Jolla, CA). All tests were two tailed, and a *P* value of <0.05 was considered significant.

RESULTS

Proteomic analysis of H. pylori strains. Previous work demonstrated that *H. pylori*-infected Mongolian gerbils fed a high-salt

TABLE 1 Comparative proteomic analysis of *H. pylori* strains[a]

Protein(s)	Gene no.[d]	No. of assigned spectral counts in strain indicated						Fold difference from input[c]			
		Expt 1[b]			Expt 2[b]			Expt 1		Expt 2	
		Input	RSO242	HSO123	Input	RSO241	HSO1	RSO242	HSO123	RSO241	HSO1
Catalase	HPB8_1087/HP0875	5	5	609	11	19	1,457	2	128	1	105
FrpB1	HPB8_1088/HP0876	9	11	110	17	20	77	1	4	1	11
FecA1	HPB8_887/HP0686	69	45	236	51	40	183	1	4	1	3
PdxA	HPB8_1634/HP1583	20	22	38	21	15	54	1	2	1	2
All		65,918	82,551	69,950	57,913	54,347	58,816				

[a] The bacteria were analyzed in a global proteomic profiling experiment (MudPIT) as described in Materials and Methods. In total, 1,175 proteins were identified.
[b] Two independent experiments were performed, with experiment 1 comparing the protein content of the input strain with that of output strains RSO242 and HSO123 and experiment 2 comparing the protein content of the input strain with that of RSO241 and HSO1.
[c] Proteins for which a minimum of 100 spectral counts were identified in both experiments 1 and 2 were analyzed to detect differences in abundance between strains.
[d] HPB8 gene numbers and the corresponding HP gene numbers in the *H. pylori* 26695 genome are listed.

diet had a higher incidence of gastric cancer than *H. pylori*-infected gerbils fed a regular-salt diet (22). In addition, infected animals fed a high-salt diet had more severe gastric inflammation, a higher gastric pH, and increased parietal cell loss than those on a regular diet (22). We hypothesized that proliferation of *H. pylori* in the intragastric environment associated with a high-salt diet might lead to the selection of strains that are optimally adapted to these conditions. To test this hypothesis, we analyzed *H. pylori* strains cultured from animals fed a regular or high-salt diet, as well as the input strain, by proteomic and whole-genome sequencing methods. A schematic detailing the experimental design and strains used for each analysis is shown in Fig. 1.

We first analyzed the proteomes of output strains cultured from two animals fed a high-salt diet (HSO1, HSO123) and two animals fed a regular-salt diet (RSO241, RSO242) with that of the input strain (see Table S1 in the supplemental material). The proteins exhibiting the greatest differences in abundance are listed in Table 1. Specifically, the two HSO strains (HSO123 and HSO1) produced higher levels of catalase (37), an iron-regulated outer membrane protein reported to bind heme and hemoglobin (FrpB1 [38, 39]), an iron-dicitrate transport protein (FecA1 [40]), and a protein involved in vitamin B_6 biosynthesis (PdxA; 4-hydroxythreonine-4-phosphate dehydrogenase [41]) than the input and RSO strains. Concordant with the results obtained at the protein level, the *katA*, *frpB1*, *fecA1*, and *pdxA* transcript levels were significantly higher in HSO1 and HSO123 than in RSO241, RSO242, and the input strain ($P < 0.05$) (Fig. 2). Thus, we detected differential abundances of several proteins and corresponding transcriptional alterations when comparing output strains from animals on a high-salt diet with the input strain and with output strains from animals on a regular diet.

Whole-genome sequence analysis. To identify mutations that might account for the differences detected in the proteomic and transcriptional analyses, we next subjected the *H. pylori* strains to whole-genome sequence analysis. We analyzed four single colonies of the input strain, four single colonies of RSO241, and four single colonies of HSO1. To facilitate the identification of differences among these strains, we aligned the sequences with the genome sequence of *H. pylori* strain B8, a closely related strain whose complete genome sequence is available (32). These analyses revealed a large number of substitution mutations, as well as insertions and deletions, many of which were detected in only a small proportion of the sequence reads from an individual single colony isolate. We focused in particular on the single-nucleotide variants

(SNVs, different from reference strain B8) that were detected in 100% of the sequence reads from at least 1 of the 12 sequenced single colonies. Table 2 lists the genetic alterations that were identified by comparing RSO241, HSO1, and the input strain with the *H. pylori* B8 reference.

As shown in Table 2, we identified three nucleotide sites (in genes encoding hypothetical protein HPB8_1463 and catalase and
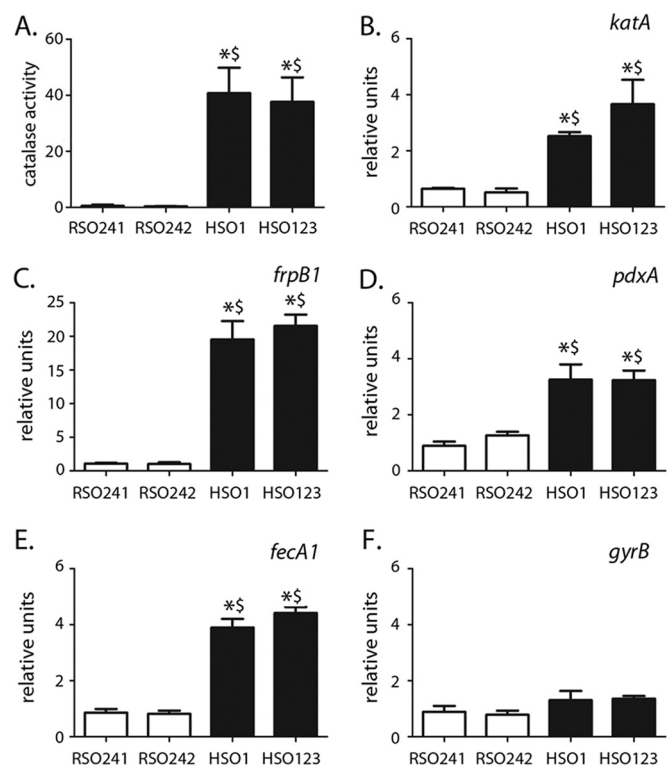

FIG 2 *H. pylori* output strains differ in catalase enzymatic activity and *katA*, *frpB1*, *pdxA*, and *fecA1* transcript levels. Four *H. pylori* output strains used in the proteomic analysis were analyzed for catalase enzymatic activity (A) and for *katA*, *frpB1*, *pdxA*, *fecA1*, and *gyrB* transcript levels (B to F) as described in Materials and Methods. Catalase enzymatic activities and transcript levels of output strains were compared to those of input strain 7.13 and are presented as relative units. The data indicate the mean ± the standard error based on at least three independent experiments. A significant difference ($P < 0.05$, Student's *t* test) in expression between the indicated HSO strain and RSO241 or RSO242 is indicated by * or $, respectively.

TABLE 2 SNVs and insertions of interest

Gene no.[b]	Protein	Position[c]	Reference[d]	SNV or insert[e]	Input[a]				RSO241[a]				HSO1[a]			
					1	2	3	4	1	2	3	4	1	2	3	4
SNVs																
HPB8_593/HP0953	Hypothetical	563546	A	G	A	A	A	A	A	A	A	A	G	G	G	G
HPB8_1139/HP1022	DNA Pol Exo	1117619	C	T	C	C	C	C	C	C	C	C	T	T	T	T
HPB8_1145/HP1027	Fur	1122559	G	A	G	G	G	G	G	G	G	G	A	A	A	A
HPB8_1463/HP0102	Hypothetical	1434104	G	A	A	A	A	G	A	A	G	A	G	G	G	G
Upstream of HPB8_1015/HP0807	FecA2	1001780	T	C	C	C	C	C	C	C	C	C	T	T	T	T
Insertion																
HPB8_1087	Catalase	Between 1064353 and 1064354	CT	CAT	CAT	CAT	CAT	CT	CAT	CAT	CAT	CT	CAT	CT	CT	CT

[a] Four single colonies of the input strain, RSO241, and HSO1 were analyzed by whole-genome sequencing. The results presented correspond to cases where 100% of the sequence reads in at least one of the sequenced samples contained the SNV or insertion indicated, which differed from the reference genome from strain B8. Shading indicates strains containing the mutation indicated.

[b] HPB8 gene numbers and the corresponding HP gene numbers in the *H. pylori* 26695 genome are provided.

[c] Position where the mutation is found in the *H. pylori* B8 genome.

[d] Nucleotide(s) present in the B8 reference genome. The nucleotides listed are those found on the coding strand of the gene indicated. CT indicates the cytosine (C) and thymine (T) nucleotides in the catalase gene (corresponding to positions 1064353 and 1064354).

[e] SNVs and insertions denote variations found in the input strain, RSO241, or HSO1 compared to the reference genome of strain B8. The insertion in the catalase gene is an adenine (A) between the C and T nucleotides.

upstream of *fecA2*) at which multiple colonies of input strain 7.13 used for these experiments differed from the B8 reference sequence. The nucleotide sequences at two of these sites (HPB8_1463 and catalase) are identical in the B8 reference sequence and a recently deposited strain 7.13 draft genome sequence (GenBank accession no. LAQK00000000) (42). Therefore, input strain 7.13 used in the present study exhibited detectable differences from the reference genome at either two or three sites, depending on which reference genome was used.

Three SNVs (in genes encoding hypothetical protein HPB8_593, DNA Pol exonuclease, and Fur) were detected in all four sequenced single colonies of the HSO1 strain but were not found in the input strain (Table 2), the B8 reference genome, or the 7.13 draft genome sequence (GenBank accession no. LAQK00000000). Two of these SNVs were nonsynonymous substitutions, and the third was a synonymous substitution. Specifically, one of the SNVs resulted in an R-to-H change at amino acid 88 of the Fur protein (R88H), another resulted in a Y-to-C change at amino acid 60 of hypothetical protein HpB8_593 (Y60C), and the third was a synonymous substitution in the gene for HpB8_1139 (DNA Pol exonuclease) (Table 2). We identified two SNVs (compared to the reference B8 strain) that were present in RSO241 and the input strain but absent from HSO1. The first of these mutations, located 29 bp upstream of the mapped *fecA2* transcriptional start site (43), was present in all four single colonies of RSO241 and all four single colonies of the input strain (Table 2). The other SNV was located three nucleotides into the ORF of a protein predicted to encode a glycosyltransferase (HpB8_1463) shown to be important for colonization of the mouse stomach (44). This mutation alters the predicted TTG translational start site to TTA (encoding leucine), which probably prevents translational initiation. This SNV was present in three of the four single colonies of RSO241 and three of the four single colonies of input strain (Table 2). We also identified a single nucleotide insertion corresponding to a frameshift mutation in the catalase gene (*katA*). This mutation was identified in three of the

four single colonies of RSO241 and three of the four single colonies of the input strain but was not identified in any of the HSO1 single colonies (Table 2).

Since two of the differentially abundant proteins identified in the proteomic analysis (catalase and FrpB1) are encoded by genes adjacent to one another on the *H. pylori* chromosome (39), we initially hypothesized that a mutation in the *katA-frpB* intergenic region might account for the alterations in the abundance of these two proteins. However, nucleotide sequence analysis did not reveal any alteration in the *katA-frpB* intergenic region that could account for the alterations in the abundance of catalase and FrpB1. The frameshift mutation in *katA* presumably accounts for the low levels of catalase detected by proteomic analysis, but we did not detect any frameshift or nonsense mutations in *frpB1* that could account for the differences in FrpB1 levels observed in the proteomic analysis. FrpB1 and two other differentially abundant proteins identified in the proteomic analysis (FecA1 and PdxA) are known to be regulated by Fur (39, 43, 45, 46), and therefore, the nonsynonymous mutation detected in *fur* could potentially account for the observed differences in the abundance of these proteins.

Genetic analysis of multiple output strains. Genome sequence analysis of four colonies of the input strain revealed that two of the polymorphisms described above (in HPB8_1463 and *katA*) were present in the input bacterial population used for gerbil infection (Table 2). In contrast, the mutations in HPB8_593, HPB8_1139, and *fur* were not found in any of the four sequenced colonies of the input strain (Table 2). The latter mutations could have arisen *in vivo* during *H. pylori* colonization of Mongolian gerbils, or alternatively, heterogeneity at these sites might have been present in the input strain used for infection of the gerbils at a low level, undetectable by sequencing of four single colonies of the input strain. As one approach for differentiating among these possibilities, we examined whether the mutations shown in Table 2 were present in output strains isolated from additional animals fed a high-salt diet or a regular diet. We used

TABLE 3 Distribution of mutations in *H. pylori* output strains

Strain	No. (%) of strains/no. of HSO in category	Inflammation score[a]	SNV[b] Fur	HPB8_593	HPB8_1139	HPB8_1463	Insertion[b] in catalase
Distribution of individual mutations							
HSO1		12	Yes	Yes	Yes	—	—
HSO123		10	Yes	Yes	Yes	—	—
HSO124		11	Yes	Yes	Yes	—	—
HSO126		11	Yes	Yes	Yes	—	—
HSO141		9	Yes	—	—	—	—
HSO147		10	Yes	Yes	Yes	—	—
HSO149		10	Yes	Yes	Yes	—	—
HSO151		11	Yes	—	—	—	—
HSO163		10	Yes	—	—	—	—
RSO1		2	Yes	Yes	—	Yes	—
RSO241		1.5	—	—	—	Yes	Yes
RSO242		7	—	—	—	Yes	Yes
RSO243		9	Yes	Yes	Yes	—	—
RSO244		10	Yes[d]	—	—	—	—
RSO251		1	—	—	—	Yes	Yes
RSO263		7	Yes	—	—	—	—
RSO266		2	Yes	—	—	—	—
RSO270		6	—	—	—	Yes	Yes
Lineages identified among input, RSO, and HSO strains[c]							
Input strain variations:							
A	1 (25)		—	—	—	—	—
B	3 (75)		—	—	—	Yes	Yes
Output group variations:							
A	7 (39)/6		Yes	Yes	Yes	—	—
B	5 (28)/3		Yes	—	—	—	—
C	4 (22)/0		—	—	—	Yes	Yes
D	1 (6)/0		Yes	Yes	—	Yes	—
E	1 (6)/0		Yes[d]	—	—	—	—

[a] Sections of gastric tissue from animals were scored for severity of total gastric inflammation on a 12-point scale that evaluated acute and chronic inflammation in both the corpus and the antrum (22).

[b] PCR was used to amplify target genes from the input 7.13 strain, nine HSO strains, and nine RSO strains with the gene-specific primers listed in Materials and Methods. "Yes" indicates the presence of SNVs or insertions that differed from the reference genome sequence of strain B8 (described in Table 2). —, no difference from reference strain B8.

[c] On the basis of the results in the top portion of the table, *H. pylori* strains (input and output) were grouped according to the distribution of the mutations identified. The number of strains and the percentage of the total number of strains in each group are presented. In addition to the total number and the percentage of the total number, the number of HSO strains belonging to each category is shown.

[d] Instead of an R88H mutation, Fur in strain RSO244 contained a P45T mutation.

gene-specific primers to PCR amplify appropriate DNA sequences from additional output strains (eight from animals on a high-salt diet and eight from animals on a low-salt diet) and sequenced the resulting amplicons.

As shown in Table 3, each of the mutations identified by whole-genome sequence analysis (Table 2) was detected in multiple additional output strains, and a second type of *fur* mutation, encoding Fur-P45T, was identified in one of the output strains (RSO244). Five output strain lineages (designated A to E) were identified on the basis of the distribution of these mutations (Table 3). One output lineage (designated C) was identical to the input strain (variation B), and the mutations defining this lineage were detected in output strains from four (22%) of the animals. The other lineages were all distinct from the input strain. Since specific mutations (including a synonymous mutation) were identified repeatedly in multiple output strains, this suggests that

some of the mutations detected in output strains may have been present in the bacterial population used to infect the gerbils. Recombination (either within the initial input strain population or subsequently within animal stomachs) presumably accounts for the emergence of multiple lineages.

We next analyzed the distribution of strain lineages and individual mutations according to the diet that the Mongolian gerbils were fed. Output lineage C (harboring the same markers as the input strain, variation B) was detected exclusively in strains cultured from animals fed a regular diet (Table 3). In contrast, lineage A was detected mainly in output strains from animals fed a high-salt diet (Table 3). The *fur-R88H* mutation was found significantly more commonly in HSO strains than in RSO strains, with *fur-R88H* found in all nine HSO strains, compared to four of the nine RSO strains (*P* = 0.0294, Fisher's exact test). The HPB8_1463 and *katA* mutations were found in five and four of the nine RSO

strains, respectively, but in none of the HSO strains ($P = 0.0294$ and $P = 0.0824$, respectively). The uneven distribution of mutations between RSO and HSO strains suggests that differential selective pressures led to the emergence of strains adapted to intragastric conditions associated with either the regular-salt or high-salt diet.

Analyses of catalase nucleotide sequences, enzymatic activity, and transcript levels. Proteomic analysis of strains HSO1 and HSO123 compared to strains RSO241 and RSO242 and the input strain revealed several differences (Table 1), including a difference in the abundance of catalase. Specifically, levels of catalase were markedly higher in strains HSO1 and HSO123 than in the input, RSO241, or RSO242 strain. Three of the four single colonies of the input strain and three of the four single colonies of RSO241 contained a frameshift mutation in *katA* (Table 2), which presumably accounts for the low levels of catalase detected by proteomic analysis. In comparison to the parental B128 human isolate and several other minimally passaged *H. pylori* human isolates, input strain 7.13 demonstrated about 200-fold lower levels of catalase activity (data not shown).

To further investigate heterogeneity in catalase production among output strains, we analyzed the catalase activity in the strains analyzed by proteomic analysis, as well as output strains from additional animals. Overall, the HSO strains demonstrated higher levels of catalase activity than the RSO strains ($P = 0.044$, Mann-Whitney test) (Fig. 3A). All nine HSO strains had markedly higher catalase activity (~40-fold higher) than the input strain (Fig. 3A). Four of the nine RSO strains had catalase activity that was similar to that of the input strain, while the remaining strains exhibited catalase activity 20- to 50-fold higher than that of the input strain. The four RSO strains with low catalase activity (RSO241, RSO242, RSO251, and RSO270) (see Fig. S1A in the supplemental material), similar to that of the WT strain, each harbored a frameshift insertional mutation in the *katA* gene (Table 2). This frameshift mutation was not detected in the remaining 14 strains (5 RSO and 9 HSO strains) with higher catalase enzymatic activity.

We next examined catalase transcript levels in the 18 output strains (Fig. 3B; see Fig. S1). There was no significant difference in *katA* transcript levels between the HSO and RSO strains (Fig. 3B, $P = 0.258$, Mann-Whitney test). Among the RSO strains, the four that contained a catalase frameshift mutation (i.e., RSO241, RSO242, RSO251, and RSO270) had low *katA* transcript levels, similar to that of the input strain (see Fig. S1). The other RSO strains with intact *katA* ORFs (RSO1, RSO243, RSO244, RSO263, and RSO266) had transcript levels, on average, about 3-fold higher than that of the input strain and similar to those of HSO strains (see Fig. S1). These results suggest that the *katA* frameshift mutation results in a reduction in *katA* transcription or *katA* transcript stability. In addition, these results suggest that there was selection for strains with a high level of catalase activity in the gastric environment associated with a high-salt diet.

Analysis of *frpB1*, *fecA1*, and *pdxA* transcript levels. The proteomic analysis revealed marked differences in the abundance of FrpB1, FecA1, and PdxA among the strains analyzed (Table 1). To further investigate this heterogeneity, we analyzed the transcription of *frpB1*, *fecA1*, and *pdxA* in the strains examined by proteomic analysis, as well as additional output strains (Fig. 3C to E). All of the HSO strains had *frpB1*, *fecA1*, and *pdxA* transcript levels that were higher than those of the input strain. In contrast, only
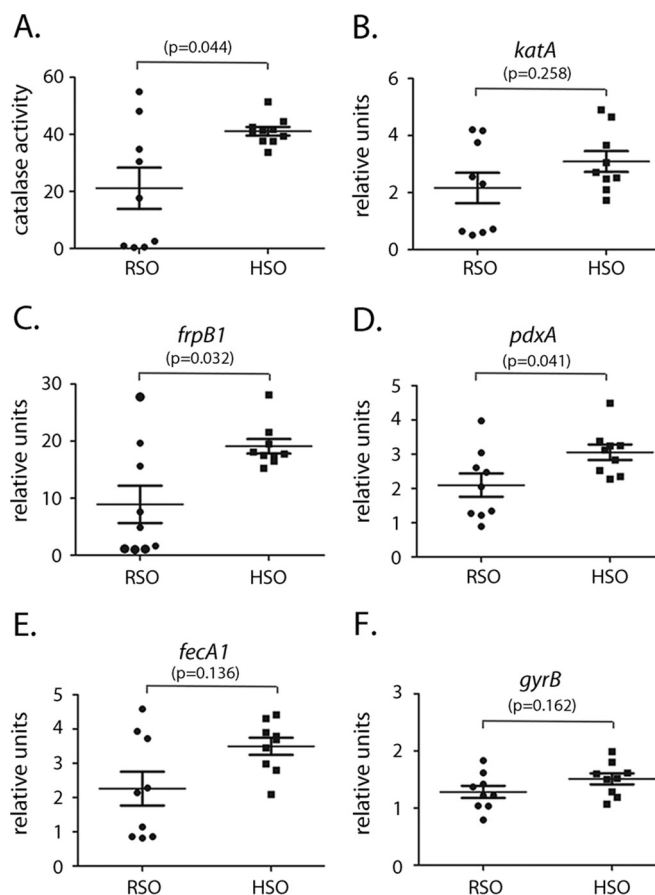

FIG 3 HSO strains demonstrate increased catalase enzymatic activity and elevated *frpB1*, *pdxA*, and *fecA1* transcript levels. Catalase enzymatic activity and transcript levels in *H. pylori* output strains from nine gerbils fed a high-salt diet and nine fed a regular-salt diet were analyzed. Graphs show catalase activity (panel A) and relative transcript units for *katA*, *frpB1*, *pdxA*, *fecA1*, and the control gene *gyrB* (panels B to F) of output strains from animals on a regular-salt (RSO) or high-salt (HSO) diet compared to those of input strain 7.13. Each data point represents the mean catalase activity or mean transcript level of each of the 18 output strains. The mean catalase activity and mean relative transcript level of each strain were calculated on the basis of at least three independent experiments. *P* values were calculated with the Mann-Whitney test.

five of the nine RSO strains (RSO1, RSO243, RSO244, RSO263, and RSO266) (see Fig. S1) had *frpB1*, *fecA1*, and *pdxA* transcript levels higher than those of the input strain; the remaining four RSO strains (RSO241, RSO242, RSO251, and RSO270) had transcript levels similar to those of the input strain. Compared to the RSO strains as a group, the HSO strains had higher *frpB1* ($P = 0.032$), *pdxA* ($P = 0.041$), and *fecA1* ($P = 0.136$) transcript levels (Fig. 3C to E). Thus, the transcriptional profiles of output strains from animals on a high-salt diet (HSO strains) differed from those of output strains from animals on a regular diet (RSO strains).

Correlation between *fur* mutations and *katA*, *frpB1*, *fecA1*, and *pdxA* transcript levels. Nucleotide sequence analyses (Tables 2 and 3) revealed the presence of a nonsynonymous *fur* mutation in all of the HSO strains, and previous studies have shown that Fur regulates the expression of *frpB1*, *fecA1*, and *pdxA* (39, 43, 45–48). Therefore, we hypothesized that the variations in Fur observed among the output strains (i.e., the WT [Fur-R88], Fur-R88H, or Fur-P45T) might account for the differences in *frpB1*, *fecA1*, and
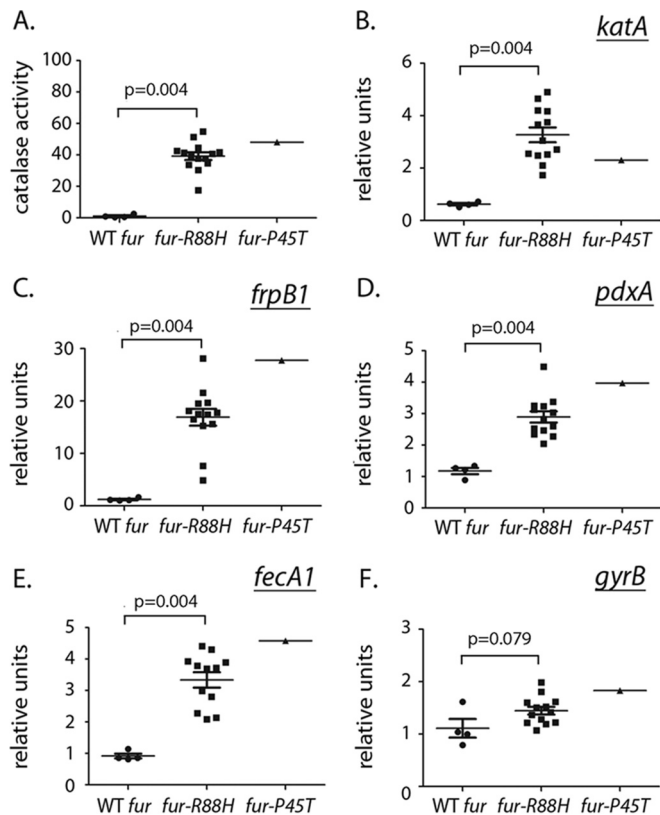
FIG 4 Analysis of output strains harboring *fur* mutations (R88H or P45T) compared to output strains harboring the WT *fur* allele. Catalase enzymatic activity and transcript levels of the 18 output strains were measured as shown in Fig. 3. The graphs show the relative catalase activity (panel A) and relative transcript units for *katA*, *frpB1*, *pdxA*, *fecA1*, and *gyrB* (panels B to F) of output strains compared to those of input strain 7.13. Data represent the mean ± the standard error of the mean based on at least three independent experiments. *P* values were calculated with the Mann-Whitney test. Output strains harboring the *fur-R88H* allele demonstrate significantly higher levels of catalase enzymatic activity and higher *katA*, *frpB1*, *fecA1*, and *pdxA* transcript levels than strains harboring the WT *fur* allele.

pdxA transcript levels. As an initial analysis, we investigated whether there was a correlation between the type of *fur* allele present and the transcript levels of these genes in the output strains. As shown in Fig. 4A to E, output strains harboring the *fur-R88H* allele demonstrated significantly higher levels of catalase enzymatic activity ($P = 0.004$), as well as higher *katA* ($P = 0.004$), *frpB1* ($P = 0.004$), *fecA1* ($P = 0.004$), and *pdxA* ($P = 0.004$) transcript levels than output strains harboring the WT *fur* allele. The RSO strain containing a *fur-P45T* allele also demonstrated higher catalase enzymatic activity and had higher *katA*, *frpB1*, *fecA1*, and *pdxA* transcript levels than output strains containing the WT *fur* allele (Fig. 4). In contrast, no significant difference in the transcript levels of the housekeeping gene *gyrB* (encoding DNA gyrase) was observed between the WT Fur and Fur-R88H mutant strains. These results supported the hypothesis that the type of *fur* allele (WT or *fur-R88H*) may account for the variation in *frpB1*, *fecA1*, *pdxA*, and possibly *katA* transcript levels among the output strains.

Functional importance of the *fur-R88H* mutation. We next sought to experimentally determine if the R88H substitution in Fur leads to altered expression of *katA*, *frpB1*, *fecA1*, and *pdxA*. Specifically, we utilized a counterselection protocol (described in

Materials and Methods) to introduce a *fur-R88H* mutation into output strain RSO251 (which contains a WT *fur* gene encoding an R88 form of Fur) (Fig. 5A). In parallel, as a control, we used the same protocol to manipulate strain RSO251 and restore the original WT R88 form of Fur (Fig. 5A). Higher expression of *frpB1*, *fecA1*, and *pdxA* was detected in the R88H mutant (shown in Fig. 5 as *fur-R88H-1*) than in the original RSO251 strain containing WT *fur* (Fig. 5B to D). As expected, the manipulated RSO251 strain in which the WT *fur* allele was restored (shown as WT *fur-1*) showed little or no increase in *frpB1*, *fecA1*, and *pdxA* transcript levels compared to the original WT RSO251 strain. The *frpB1* and *pdxA* transcript levels of the *fur-R88H-1* strain were significantly higher than those of the strain with restored WT Fur ($P = 0.027$) (Fig. 5B and C) but were lower than the corresponding levels detected in a Δ*fur* mutant. No difference in the expression of *katA* (Fig. 5E) or the housekeeping gene (*gyrB* for DNA gyrase) (Fig. 5F) was detected when the *fur* mutant strains were compared with strains containing WT *fur*, indicating that Fur does not regulate the expression of either *katA* or *gyrB*. A similar mutagenesis approach was carried out with input strain 7.13 (which encodes WT Fur-R88), and similar results were obtained (Fig. 5G to I). These data indicate that the association between the *fur-R88H* mutation and *katA* transcript levels shown in Fig. 4 is not directly attributable to an alteration in *fur* but instead is attributed to the frameshift mutation in *katA* that was present in the four RSO strains containing WT *fur*.

As another approach to assess the effect of the R88H mutation on *frpB1* expression, we reintroduced the WT *fur* allele into the RSO251 strain encoding Fur-R88H (i.e., *fur-R88H-1*, Fig. 6) as described in Materials and Methods and the legend to Fig. 6. The *frpB1* transcript levels in strains designated WT *fur-1*, *fur-R88H-1*, WT *fur-2*, *fur-R88H-2*, and Δ*fur1* (Fig. 6A) were compared to that in the original RSO251 output strain. Consistent with the results shown in Fig. 5, the strain harboring the mutated *fur-R88H* allele (strain *fur-R88H-1*) expressed higher levels of *frpB1* than the WT *fur-1* strain ($P < 0.05$), but the levels of *frpB1* expression were lower than those detected in Δ*fur1* (the *fur* null mutant) (Fig. 6B). When WT *fur* was introduced into the Δ*fur1* null mutant strain (resulting in WT *fur-2*), *frpB1* transcript levels were reduced to levels similar to those found in the WT *fur-1* strain. In contrast, when *fur-R88H* was introduced into the Δ*fur1* mutant (resulting in *fur-R88H-2*), *frpB1* transcript levels were similar to those found in strain *fur-R88H-1*. These results provided further evidence that the Fur-R88H mutation influences the levels of *frpB1* transcription.

Strains producing Fur-R88H are more resistant to salt and oxidative stress. Previous studies have shown that *H. pylori fur* mutant strains demonstrate a growth defect at elevated salt concentrations compared to the WT strain (49), and several Fur-regulated genes (e.g., *napA* and *sodB*) are involved in oxidative-stress resistance in *H. pylori* (50–54). Therefore, we hypothesized that the *fur-R88H* mutation might affect the ability of *H. pylori* to grow in either an oxidative-stress environment induced by paraquat (36) or medium containing elevated salt concentrations. In initial experiments (Fig. 7A), we introduced a kanamycin resistance marker (*aph3*) into strain RSO251-WT *fur-1* (producing WT Fur) and a chloramphenicol resistance marker (*cat*) into strain RSO251-*fur-R88H-1* (Fig. 6A). To allow simultaneous and direct comparison of the effects of either NaCl or paraquat on WT and *fur*-R88H bacteria, a condition reflective of the competition
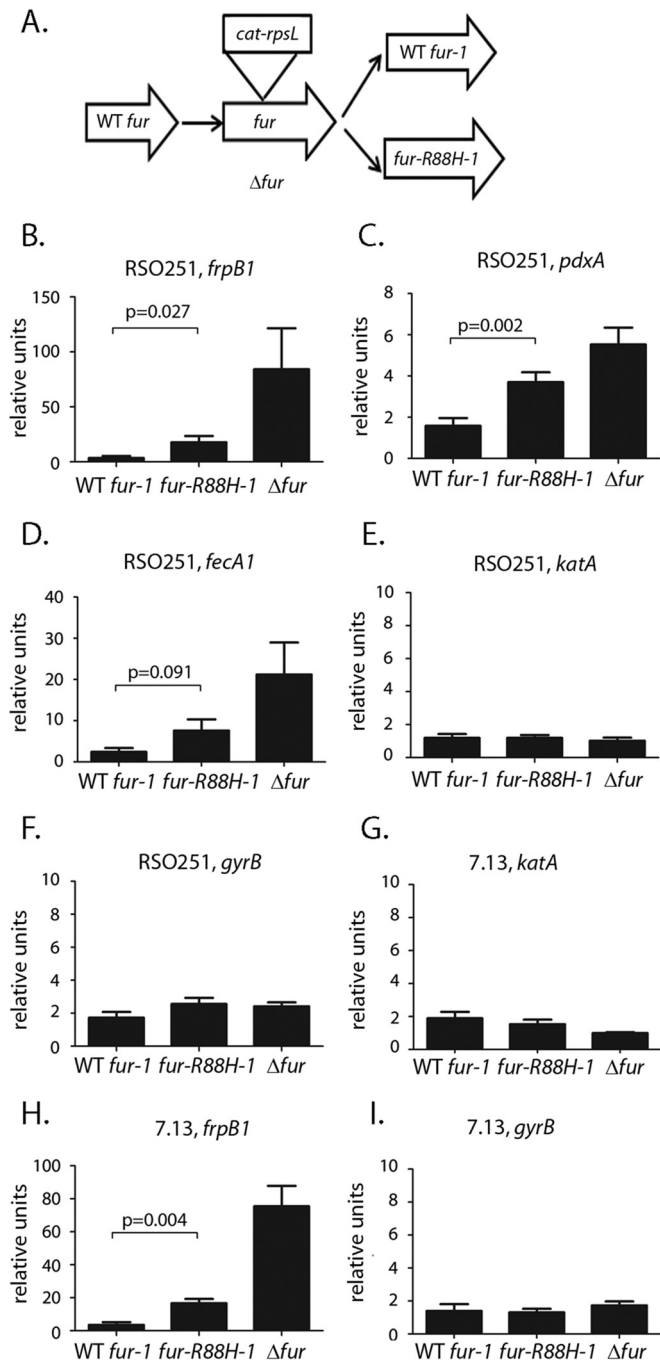
FIG 5 Introduction of a *fur-R88H* mutation into RSO251 or input strain 7.13 alters the expression of *katA*, *frpB1*, *pdxA*, and *fecA1*. The *fur* gene in *H. pylori* strain RSO251 (output strain containing a WT *fur* allele and intact catalase activity) and input strain 7.13 (containing WT *fur* and low catalase activity) was subjected to mutagenesis as shown in panel A. Introduction of a *cat-rpsL* cassette into *fur* resulted in a Δ*fur* mutant strain. Subsequently, the *cat-rpsL* cassette was replaced with an intact copy of either WT *fur* or *fur-R88H* (designated *fur-1* or *fur-R88H-1*). Panels B to F show transcriptional analysis of the genes indicated in strains derived from RSO251, and panels G to I show an analysis of strains derived from input strain 7.13. The transcript levels in panels B to F are compared to those of the nonmutated RSO251 strain, and the transcript levels in panels G to I are compared to those of input strain 7.13 (expressed in relative units). Data represent the mean ± the standard error based on at least three independent experiments. *P* values were calculated with Student's *t* test.
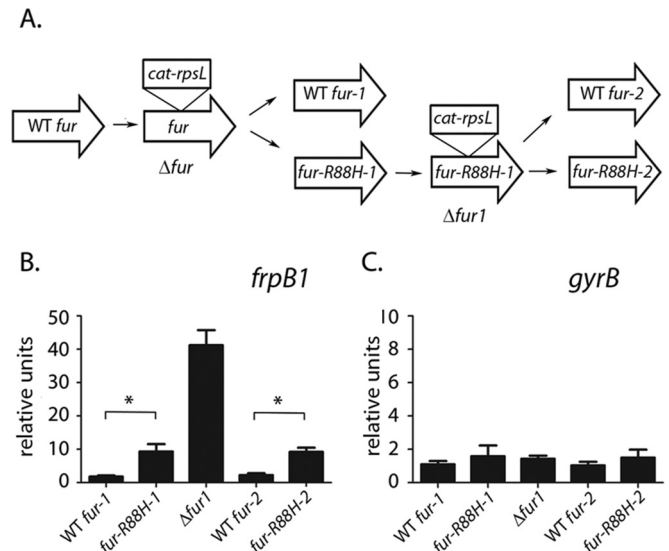

FIG 6 Introduction of a WT *fur* allele into a strain harboring a *fur-R88H* allele reduces expression of *frpB1*. The *fur* allele in *H. pylori* strain RSO251 (containing a WT *fur* allele and intact catalase activity) was mutated as described in Fig. 5A, and further mutagenesis steps were conducted as illustrated in panel A. These further mutagenesis steps resulted in the replacement of the *fur-R88H* allele (*fur-R88H-1*) with either a WT *fur* allele (WT *fur-2*) or a reintroduced copy of *fur-R88H* (*fur-R88H-2*) as a control. The *frpB1* and *gyrB* transcript levels in each strain are compared to the levels in the nonmutated RSO251 strain (presented as relative units). Results are the mean ± the standard error of the mean based on at least three independent experiments. *P* values were calculated with Student's *t* test. *, $P < 0.05$.

that occurs within the stomach, we performed competition assays. The marked strains were coinoculated (at equivalent optical densities) into three liquid media: brucella broth without additives, brucella broth with an elevated NaCl concentration (1.2% NaCl), and brucella broth containing paraquat. After growth overnight, the cultures were plated on medium containing kanamycin or chloramphenicol to select for bacteria containing WT *fur* or *fur-R88H*, respectively, and the numbers of CFU per milliliter of culture were determined. As shown in Fig. 7A, the composition of the bacterial population from overnight cultures in brucella broth without additives was about 55% *fur-R88H* (2.8×10^7 CFU/ml) and 45% WT *fur* (2.1×10^7 CFU/ml). When the bacteria were cultured in brucella broth containing paraquat, *fur-R88H* bacteria constituted about 90% of the population ($P < 0.05$) (Fig. 7A). Bacteria harboring WT *fur* and *fur-R88H* were each susceptible to the effects of paraquat, leading to a reduction in the numbers of viable bacteria (3.5×10^6 CFU/ml *fur-R88H* and 2.7×10^5 CFU/ml WT *fur* cultured in paraquat-containing medium). When the coculture experiments were performed with high-salt medium, the *fur-R88H* containing bacteria again made up about 90% of the population (Fig. 7A), corresponding to 2×10^7 CFU/ml *fur-R88H*-containing bacteria and 2.2×10^6 CFU/ml WT *fur*-containing bacteria, respectively. These results indicated that bacteria containing the *fur-R88H* allele are more resistant to the effects of paraquat and high salt concentrations than are bacteria harboring the WT *fur* allele.

To ensure that the choice of antibiotic marker did not affect the outcome of the assays, we reversed the antibiotic markers and performed coculture experiments with RSO251 WT *fur1* bacteria
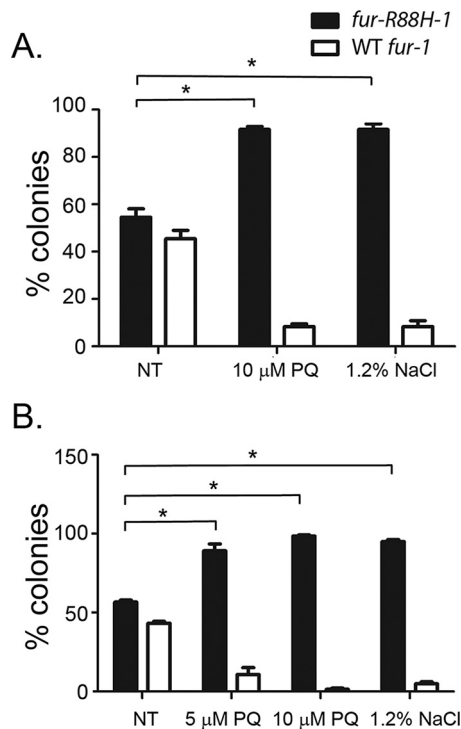
FIG 7 Effects of paraquat (PQ) and an increased sodium chloride concentration on the growth of *H. pylori* strains harboring WT *fur* or the *fur-R88H* allele. RSO251 strains harboring either WT *fur* (*fur-1*) or the *fur-R88H-1* allele were generated as shown in Fig. 5A. The bacteria were then tagged by the introduction of antibiotic markers (a *cat* [chloramphenicol acetyltransferase] or *aph3* cassette) into the *ureA* locus. Competition assays were performed by inoculating equal numbers of the two bacterial strains into medium containing paraquat (5 or 10 μM) or 1.2% NaCl and culturing them for 15 h. The cultures were then plated on BB-FBS plates containing either kanamycin or chloramphenicol. Panel A illustrates results of competition experiments in which a strain harboring the WT *fur* allele was tagged with an *aph3* cassette and a strain harboring the *fur-R88H* allele was tagged with a *cat* cassette. Panel B illustrates results of experiments in which a strain harboring the WT *fur* allele was tagged with a *cat* cassette and a strain harboring the *fur-R88H* allele was tagged with an *aph3* cassette. Results represent the mean ± the standard error of the mean based on at least three independent experiments. Percentages of colonies producing either WT Fur or Fur-R88H after overnight selection are shown. *, $P <$ 0.05 (Student's *t* test). NT, no treatment.

tagged with a *cat* cassette and RSO251 *fur-R88H-1* bacteria tagged with an *aph3* cassette. When grown in brucella broth without additives, *fur-R88H* and WT *fur* bacteria made up approximately 52 and 48% of the total population recovered (4.3 × 10^8 and 3.2 × 10^8 CFU/ml, respectively) (Fig. 7B). When the bacteria were cultured in the presence of 5 or 10 μM paraquat, *furR-R88H*-containing bacteria constituted 90 or 99% of the populations, respectively (Fig. 7B). Specifically, in the presence of 5 or 10 μM paraquat, 3.1 × 10^8 and 1.6 × 10^7 CFU/ml of *fur-R88H* bacteria were recovered and 3.1 × 10^7 and 6.9 × 10^5 CFU/ml of WT *fur* bacteria were recovered, respectively. When the cocultures were performed with high-salt medium, the *fur-R88H*-containing bacteria constituted about 95% of the population (Fig. 7B), corresponding to 4.8 × 10^8 CFU/ml (*furR-88H*) and 3 × 10^7 CFU/ml (WT *fur*), respectively. These results indicate that *H. pylori* strains expressing Fur-R88H are more resistant to oxidative stress and elevated salt concentrations than are *H. pylori* strains producing WT Fur.

DISCUSSION

In this study, we tested the hypothesis that the evolution of *H. pylori* within a host can be influenced by the composition of the diet. Specifically, we hypothesized that the altered gastric environment generated by a high-salt diet might promote the selection of *H. pylori* strains adapted to these gastric conditions. To test this hypothesis, we analyzed *H. pylori* strains isolated from experimentally infected Mongolian gerbils that were fed either a high-salt diet or a regular-salt diet over a 4-month time period. Proteomic, transcriptional, and nucleotide sequence analyses revealed multiple differences between output strains from animals fed a high-salt diet and output strains from animals on a regular-salt diet.

The mutations detected in the output strains (Table 2) could potentially have arisen *in vivo*. Alternatively, since we detected evidence of genetic heterogeneity in the *H. pylori* population that was administered to gerbils, some of the mutations were probably already present in the *H. pylori* input population prior to the start of the animal experiments. Regardless of the time point when these mutations first arose, the results of this study provide evidence that there was positive selection of specific *H. pylori* variants during the course of infection. We propose that certain variants have increased fitness for proliferation in the gastric environment associated with a high-salt diet than in the gastric environment associated with a regular-salt diet. As described previously, these two types of gastric environments differ in multiple features (22). In addition to the differences in gastric luminal salt concentrations, the *H. pylori*-infected animals fed a high-salt diet had lower levels of gastric acidity and higher levels of gastric inflammation than infected animals fed a regular-salt diet (22). At present, it is not possible to determine whether the high-salt diet was directly responsible for the observed selection of *H. pylori* variants or whether the effect of a high-salt diet was indirect (for example, due to different levels of gastric inflammation or differences in pH). Similarly, at present, it is not possible to determine if there was a single dominant selective pressure or if the selection resulted from a combination of multiple environmental pressures. Human diets vary considerably in salt content (as well as in many other ways). Therefore, we presume that similar selection of *H. pylori* variants occurs continually in humans in response to the composition of their diet. The present results suggest that variation in the composition of the human diet may be an important factor that influences the evolution of *H. pylori* in individual human stomachs.

Proteomic analysis of representative strains revealed higher levels of KatA, FrpB1, FecA1, and PdxA in the HSO strains than in the RSO strains and the input strain. The differences in the abundance of FrpB1, FecA1, and PdxA were attributable to transcriptional differences, and the difference in the abundance of KatA was attributable primarily to a frameshift mutation in the catalase gene. Genome sequence analysis of representative strains revealed the presence of multiple polymorphisms in an HSO strain compared to RSO and input strains, including a *fur-R88H* mutation, an alteration in the catalase gene resulting in the correction of a frameshift mutation, a mutation encoding a Y60C substitution in the hypothetical protein HPB8_593, and a TTG-to-TTA mutation that may affect the initiation of the translation of a predicted glycosyltransferase, HPB8_1463. These mutations were distributed nonrandomly in HSO strains compared to RSO strains (Table 2). For example, the *fur-R88H* mutation was identified in HSO strains significantly more commonly than in RSO strains.

Experimental studies provided evidence that the Fur-R88H mutation accounts for the altered expression of *frpB1*, *fecA1*, and *pdxA*. Like Fur in other bacterial species, *H. pylori* Fur can, in the presence of ferrous iron, repress transcription by binding *fur* box sequences upstream of target genes. *frpB1*, *fecA1*, and *pdxA* are examples of *H. pylori* genes repressed by iron-bound Fur (39, 43, 45–48). The Fur R88H and P45T mutations are each located close to Fur amino acid residues important for iron coordination of Fur (E90 and H42, respectively) (55), and therefore, we speculate that these mutations might affect the ability of Fur to regulate its target genes. Consistent with this hypothesis, several mutations close to Fur R88 (e.g., R87Q, Y89C, and E90Q) are known to impair Fur regulatory activity (56). Although substitution mutations at the Fur R88 position are not found commonly in *H. pylori* isolates from humans, an R88H mutation identical to the mutation observed in the present study has been detected in at least three *H. pylori* isolates from humans (57).

Previous studies have shown that *H. pylori* Fur has a role in resistance to high-salt conditions (49) and resistance to oxidative stress (50–54) and contributes to *H. pylori* colonization of the stomach (58). To further investigate the functional consequences of the Fur-R88H mutation, we compared the abilities of *H. pylori* strains producing either WT Fur or Fur-R88H to grow in medium containing elevated salt concentrations or in oxidative-stress environments. Under both conditions, *H. pylori* strains expressing Fur-R88H exhibited a competitive advantage over strains expressing WT Fur. The exact mechanisms by which the R88H mutation influences these two phenotypes is not yet known, but there are several likely possibilities. For example, since Fur-R88H-producing strains express higher levels of iron transport proteins FrpB1 and FecA1, we speculate that these strains might acquire iron more efficiently than strains producing WT Fur. Since iron functions as a cofactor for oxidative-stress enzymes such as catalase and SodB, increased iron uptake in Fur-R88H-producing strains might lead to increased survival of *H. pylori* under oxidative-stress conditions. The mechanisms by which the R88H mutation contributes to increased salt resistance are less clear. Previous studies of *Bacillus subtilis* and *B. cereus* suggested a link between bacterial stress responses to high-salt conditions and oxidative stress (59, 60). For instance, salt stress has been reported to induce the production of proteins that allow cross-protection against both oxidative stress and salt stress (59, 60). Thus, it is possible that *H. pylori* utilizes the same stress response when it encounters either elevated salt concentrations or oxidative stress. This idea is supported by the fact that Fur has been proposed to be a global regulator in *H. pylori*, responding to diverse stimuli such as iron limitation, low pH, oxidative stress, and salt stress (46, 49, 51). Alternatively, exposure of the bacteria to high salt concentrations could result in oxidative stress (59) or could affect the bioavailability of iron to the bacteria. For example, studies with *Bacillus* have shown that high-salt conditions reduced iron availability, resulting in the upregulated expression of genes required for siderophore synthesis and iron uptake systems, through a Fur-dependent process (61). Moreover, high-salt conditions retarded *B. subtilis* growth, an effect that was partially reversed by the addition of excess iron to the growth medium (61). An enhanced ability of the strain containing Fur-R88H to scavenge iron through increased expression of iron uptake enzymes might confer a survival advantage under high-salt conditions.

The consumption of high levels of dietary salt has been associated with an increased risk of gastric cancer in human populations (14), and we demonstrated previously that *H. pylori*-infected Mongolian gerbils fed a high-salt diet were more likely to develop gastric cancer than were infected animals fed a regular-salt diet (22). The present results provide evidence that the evolution of *H. pylori* is influenced by the composition of the diet and that a high-salt diet leads to the selection of strains that differ from strains present in animals on a regular-salt diet. Only a small number of mutations were identified in the present study because of the relatively short time period in which animals were fed the different diets and because output strains from only two animals were subjected to whole-genome sequence analysis. Presumably, the composition of the diet would have an even greater detectable impact on the evolution of *H. pylori* if longer periods of time and strains from larger numbers of animals were studied. The most striking genetic change detected in the present study resulted in altered levels of proteins involved in iron acquisition and oxidative-stress resistance, but the composition of the diet could potentially have a much broader impact on the evolution of *H. pylori*. We speculate that the adaptation of *H. pylori* strains to the gastric environment associated with a high-salt diet may concomitantly result in the emergence of strains that have an increased carcinogenic potential.

ACKNOWLEDGMENTS

REFERENCES

1. **Atherton JC, Blaser MJ.** 2009. Coadaptation of *Helicobacter pylori* and humans: ancient history, modern implications. J Clin Invest **119:**2475–2487. http://dx.doi.org/10.1172/JCI38605.

2. **Cover TL, Blaser MJ.** 2009. *Helicobacter pylori* in health and disease. Gastroenterology **136:**1863–1873. http://dx.doi.org/10.1053/j.gastro.2009.01.073.

3. **Blaser MJ, Berg DE.** 2001. *Helicobacter pylori* genetic diversity and risk of human disease. J Clin Invest **107:**767–773. http://dx.doi.org/10.1172/JCI12672.

4. **Suerbaum S, Josenhans C.** 2007. *Helicobacter pylori* evolution and phenotypic diversification in a changing host. Nat Rev Microbiol **5:**441–452. http://dx.doi.org/10.1038/nrmicro1658.

5. **Falush D, Kraft C, Taylor NS, Correa P, Fox JG, Achtman M, Suerbaum S.** 2001. Recombination and mutation during long-term gastric colonization by *Helicobacter pylori:* estimates of clock rates, recombination size, and minimal age. Proc Natl Acad Sci U S A **98:**15056–15061. http://dx.doi.org/10.1073/pnas.251396098.

6. **Linz B, Windsor HM, McGraw JJ, Hansen LM, Gajewski JP, Tomsho LP, Hake CM, Solnick JV, Schuster SC, Marshall BJ.** 2014. A mutation burst during the acute phase of *Helicobacter pylori* infection in humans and rhesus macaques. Nat Commun **5:**4165.

7. **Amieva MR, El-Omar EM.** 2008. Host-bacterial interactions in *Helicobacter pylori* infection. Gastroenterology **134:**306–323. http://dx.doi.org/10.1053/j.gastro.2007.11.009.

8. **Fox JG, Wang TC.** 2007. Inflammation, atrophy, and gastric cancer. J Clin Invest **117:**60–69. http://dx.doi.org/10.1172/JCI30111.

9. **Blaser MJ, Perez-Perez GI, Kleanthous H, Cover TL, Peek RM, Chyou PH, Stemmermann GN, Nomura A.** 1995. Infection with *Helicobacter pylori* strains possessing *cagA* is associated with an increased risk of developing adenocarcinoma of the stomach. Cancer Res **55:**2111–2115.

10. Hatakeyama M. 2014. *Helicobacter pylori* CagA and gastric cancer: a paradigm for hit-and-run carcinogenesis. Cell Host Microbe **15**:306–316. http://dx.doi.org/10.1016/j.chom.2014.02.008.

11. Fischer W, Puls J, Buhrdorf R, Gebert B, Odenbreit S, Haas R. 2001. Systematic mutagenesis of the *Helicobacter pylori cag* pathogenicity island: essential genes for CagA translocation in host cells and induction of interleukin-8. Mol Microbiol **42**:1337–1348.

12. Atherton JC, Cao P, Peek RM, Jr, Tummuru MK, Blaser MJ, Cover TL. 1995. Mosaicism in vacuolating cytotoxin alleles of *Helicobacter pylori*. Association of specific *vacA* types with cytotoxin production and peptic ulceration. J Biol Chem **270**:17771–17777.

13. Figueiredo C, Machado JC, Pharoah P, Seruca R, Sousa S, Carvalho R, Capelinha AF, Quint W, Caldas C, van Doorn LJ, Carneiro F, Sobrinho-Simoes M. 2002. *Helicobacter pylori* and interleukin 1 genotyping: an opportunity to identify high-risk individuals for gastric carcinoma. J Natl Cancer Inst **94**:1680–1687. http://dx.doi.org/10.1093/jnci/94.22.1680.

14. Cover TL, Peek RM, Jr. 2013. Diet, microbial virulence, and *Helicobacter pylori*-induced gastric cancer. Gut Microbes **4**:482–493. http://dx.doi.org/10.4161/gmic.26262.

15. Lee SA, Kang D, Shim KN, Choe JW, Hong WS, Choi H. 2003. Effect of diet and *Helicobacter pylori* infection to the risk of early gastric cancer. J Epidemiol **13**:162–168. http://dx.doi.org/10.2188/jea.13.162.

16. Tsugane S. 2005. Salt, salted food intake, and risk of gastric cancer: epidemiologic evidence. Cancer Sci **96**:1–6. http://dx.doi.org/10.1111/j.1349-7006.2005.00006.x.

17. Tsugane S, Sasazuki S. 2007. Diet and the risk of gastric cancer: review of epidemiological evidence. Gastric Cancer **10**:75–83. http://dx.doi.org/10.1007/s10120-007-0420-0.

18. Bergin IL, Sheppard BJ, Fox JG. 2003. *Helicobacter pylori* infection and high dietary salt independently induce atrophic gastritis and intestinal metaplasia in commercially available outbred Mongolian gerbils. Dig Dis Sci **48**:475–485. http://dx.doi.org/10.1023/A:1022524313355.

19. Fox JG, Dangler CA, Taylor NS, King A, Koh TJ, Wang TC. 1999. High-salt diet induces gastric epithelial hyperplasia and parietal cell loss, and enhances *Helicobacter pylori* colonization in C57BL/6 mice. Cancer Res **59**:4823–4828.

20. Gamboa-Dominguez A, Ubbelohde T, Saqui-Salces M, Romano-Mazzoti L, Cervantes M, Dominguez-Fonseca C, de la Luz Estreber M, Ruiz-Palacios GM. 2007. Salt and stress synergize *Helicobacter pylori*-induced gastric lesions, cell proliferation, and p21 expression in Mongolian gerbils. Dig Dis Sci **52**:1517–1526. http://dx.doi.org/10.1007/s10620-006-9524-3.

21. Kato S, Tsukamoto T, Mizoshita T, Tanaka H, Kumagai T, Ota H, Katsuyama T, Asaka M, Tatematsu M. 2006. High salt diets dose-dependently promote gastric chemical carcinogenesis in *Helicobacter pylori*-infected Mongolian gerbils associated with a shift in mucin production from glandular to surface mucous cells. Int J Cancer **119**:1558–1566. http://dx.doi.org/10.1002/ijc.21810.

22. Gaddy JA, Radin JN, Loh JT, Zhang F, Washington MK, Peek RM, Jr, Algood HM, Cover TL. 2013. High dietary salt intake exacerbates *Helicobacter pylori*-induced gastric carcinogenesis. Infect Immun **81**:2258–2267. http://dx.doi.org/10.1128/IAI.01271-12.

23. Gancz H, Jones KR, Merrell DS. 2008. Sodium chloride affects *Helicobacter pylori* growth and gene expression. J Bacteriol **190**:4100–4105. http://dx.doi.org/10.1128/JB.01728-07.

24. Loh JT, Friedman DB, Piazuelo MB, Bravo LE, Wilson KT, Peek RM, Jr, Correa P, Cover TL. 2012. Analysis of *Helicobacter pylori cagA* promoter elements required for salt-induced upregulation of CagA expression. Infect Immun **80**:3094–3106. http://dx.doi.org/10.1128/IAI.00232-12.

25. Loh JT, Torres VJ, Cover TL. 2007. Regulation of *Helicobacter pylori cagA* expression in response to salt. Cancer Res **67**:4709–4715. http://dx.doi.org/10.1158/0008-5472.CAN-06-4746.

26. Voss BJ, Loh JT, Hill S, Rose KL, McDonald HW, Cover TL. 24 June 2015. Alteration of the *Helicobacter pylori* membrane proteome in response to changes in environmental salt concentration. Proteomics Clin Appl http://dx.doi.org/10.1002/prca.201400176.

27. Franco AT, Israel DA, Washington MK, Krishna U, Fox JG, Rogers AB, Neish AS, Collier-Hyams L, Perez-Perez GI, Hatakeyama M, Whitehead R, Gaus K, O'Brien DP, Romero-Gallo J, Peek RM, Jr. 2005. Activation of beta-catenin by carcinogenic *Helicobacter pylori*. Proc Natl Acad Sci U S A **102**:10646–10651. http://dx.doi.org/10.1073/pnas.0504927102.

28. Israel DA, Salama N, Arnold CN, Moss SF, Ando T, Wirth HP, Tham KT, Camorlinga M, Blaser MJ, Falkow S, Peek RM, Jr. 2001. *Helicobacter pylori* strain-specific differences in genetic content, identified by microarray, influence host inflammatory responses. J Clin Invest **107**:611–620. http://dx.doi.org/10.1172/JCI11450.

29. Voss BJ, Gaddy JA, McDonald WH, Cover TL. 2014. Analysis of surface-exposed outer membrane proteins in *Helicobacter pylori*. J Bacteriol **196**:2455–2471. http://dx.doi.org/10.1128/JB.01768-14.

30. MacCoss MJ, McDonald WH, Saraf A, Sadygov R, Clark JM, Tasto JJ, Gould KL, Wolters D, Washburn M, Weiss A, Clark JI, Yates JR, III. 2002. Shotgun identification of protein modifications from protein complexes and lens tissue. Proc Natl Acad Sci U S A **99**:7900–7905. http://dx.doi.org/10.1073/pnas.122231399.

31. Shaffer CL, Gaddy JA, Loh JT, Johnson EM, Hill S, Hennig EE, McClain MS, McDonald WH, Cover TL. 2011. *Helicobacter pylori* exploits a unique repertoire of type IV secretion system components for pilus assembly at the bacteria-host cell interface. PLoS Pathog **7**:e1002237. http://dx.doi.org/10.1371/journal.ppat.1002237.

32. Farnbacher M, Jahns T, Willrodt D, Daniel R, Haas R, Goesmann A, Kurtz S, Rieder G. 2010. Sequencing, annotation, and comparative genome analysis of the gerbil-adapted *Helicobacter pylori* strain B8. BMC Genomics **11**:335. http://dx.doi.org/10.1186/1471-2164-11-335.

33. Barrozo RM, Cooke CL, Hansen LM, Lam AM, Gaddy JA, Johnson EM, Cariaga TA, Suarez G, Peek RM, Jr, Cover TL, Solnick JV. 2013. Functional plasticity in the type IV secretion system of *Helicobacter pylori*. PLoS Pathog **9**:e1003189. http://dx.doi.org/10.1371/journal.ppat.1003189.

34. Styer CM, Hansen LM, Cooke CL, Gundersen AM, Choi SS, Berg DE, Benghezal M, Marshall BJ, Peek RM, Jr, Boren T, Solnick JV. 2010. Expression of the BabA adhesin during experimental infection with *Helicobacter pylori*. Infect Immun **78**:1593–1600. http://dx.doi.org/10.1128/IAI.01297-09.

35. Johnson EM, Gaddy JA, Voss BJ, Hennig EE, Cover TL. 2014. Genes required for assembly of pili associated with the *Helicobacter pylori cag* type IV secretion system. Infect Immun **82**:3457–3470. http://dx.doi.org/10.1128/IAI.01640-14.

36. Waidner B, Greiner S, Odenbreit S, Kavermann H, Velayudhan J, Stahler F, Guhl J, Bisse E, van Vliet AH, Andrews SC, Kusters JG, Kelly DJ, Haas R, Kist M, Bereswill S. 2002. Essential role of ferritin Pfr in *Helicobacter pylori* iron metabolism and gastric colonization. Infect Immun **70**:3923–3929. http://dx.doi.org/10.1128/IAI.70.7.3923-3929.2002.

37. Odenbreit S, Wieland B, Haas R. 1996. Cloning and genetic characterization of *Helicobacter pylori* catalase and construction of a catalase-deficient mutant strain. J Bacteriol **178**:6960–6967.

38. Carrizo-Chávez MA, Cruz-Castaneda A, Olivares-Trejo Jde J. 2012. The *frpB1* gene of *Helicobacter pylori* is regulated by iron and encodes a membrane protein capable of binding haem and haemoglobin. FEBS Lett **586**:875–879. http://dx.doi.org/10.1016/j.febslet.2012.02.015.

39. Delany I, Pacheco AB, Spohn G, Rappuoli R, Scarlato V. 2001. Iron-dependent transcription of the *frpB* gene of *Helicobacter pylori* is controlled by the Fur repressor protein. J Bacteriol **183**:4932–4937. http://dx.doi.org/10.1128/JB.183.16.4932-4937.2001.

40. Tsugawa H, Suzuki H, Matsuzaki J, Hirata K, Hibi T. 2012. FecA1, a bacterial iron transporter, determines the survival of *Helicobacter pylori* in the stomach. Free Radic Biol Med **52**:1003–1010. http://dx.doi.org/10.1016/j.freeradbiomed.2011.12.011.

41. Grubman A, Phillips A, Thibonnier M, Kaparakis-Liaskos M, Johnson C, Thiberge JM, Radcliff FJ, Ecobichon C, Labigne A, de Reuse H, Mendz GL, Ferrero RL. 2010. Vitamin B6 is required for full motility and virulence in *Helicobacter pylori*. mBio **1**:e00112–10. http://dx.doi.org/10.1128/mBio.00112-10.

42. Asim M, Chikara SK, Ghosh A, Vudathala S, Romero-Gallo J, Krishna US, Wilson KT, Israel DA, Peek RM, Jr, Chaturvedi R. 2015. Draft genome sequence of gerbil-adapted carcinogenic *Helicobacter pylori* strain 7.13. Genome Announc **3**:e00641–15. http://dx.doi.org/10.1128/genomeA.00641-15.

43. Danielli A, Romagnoli S, Roncarati D, Costantino L, Delany I, Scarlato V. 2009. Growth phase and metal-dependent transcriptional regulation of the *fecA* genes in *Helicobacter pylori*. J Bacteriol **191**:3717–3725. http://dx.doi.org/10.1128/JB.01741-08.

44. Baldwin DN, Shepherd B, Kraemer P, Hall MK, Sycuro LK, Pinto-Santini DM, Salama NR. 2007. Identification of *Helicobacter pylori* genes that contribute to stomach colonization. Infect Immun **75**:1005–1016. http://dx.doi.org/10.1128/IAI.01176-06.

45. Ernst FD, Bereswill S, Waidner B, Stoof J, Mader U, Kusters JG, Kuipers EJ, Kist M, van Vliet AH, Homuth G. 2005. Transcriptional

profiling of *Helicobacter pylori* Fur- and iron-regulated gene expression. Microbiology **151**:533–546. http://dx.doi.org/10.1099/mic.0.27404-0.

46. **Gancz H, Censini S, Merrell DS.** 2006. Iron and pH homeostasis intersect at the level of Fur regulation in the gastric pathogen *Helicobacter pylori*. Infect Immun **74**:602–614. http://dx.doi.org/10.1128/IAI.74.1.602-614.2006.

47. **Agriesti F, Roncarati D, Musiani F, Del Campo C, Iurlaro M, Sparla F, Ciurli S, Danielli A, Scarlato V.** 2014. FeON-FeOFF: the *Helicobacter pylori* Fur regulator commutates iron-responsive transcription by discriminative readout of opposed DNA grooves. Nucleic Acids Res **42**:3138–3151. http://dx.doi.org/10.1093/nar/gkt1258.

48. **Danielli A, Roncarati D, Delany I, Chiarini V, Rappuoli R, Scarlato V.** 2006. In vivo dissection of the *Helicobacter pylori* Fur regulatory circuit by genome-wide location analysis. J Bacteriol **188**:4654–4662. http://dx.doi.org/10.1128/JB.00120-06.

49. **Gancz H, Merrell DS.** 2011. The *Helicobacter pylori* ferric uptake regulator (Fur) is essential for growth under sodium chloride stress. J Microbiol **49**:294–298. http://dx.doi.org/10.1007/s12275-011-0396-7.

50. **Carpenter BM, Gancz H, Gonzalez-Nieves RP, West AL, Whitmire JM, Michel SL, Merrell DS.** 2009. A single nucleotide change affects *fur*-dependent regulation of *sodB* in *Helicobacter pylori*. PLoS One **4**:e5369. http://dx.doi.org/10.1371/journal.pone.0005369.

51. **Cooksley C, Jenks PJ, Green A, Cockayne A, Logan RP, Hardie KR.** 2003. NapA protects *Helicobacter pylori* from oxidative stress damage, and its production is influenced by the ferric uptake regulator. J Med Microbiol **52**:461–469. http://dx.doi.org/10.1099/jmm.0.05070-0.

52. **Ernst FD, Homuth G, Stoof J, Mader U, Waidner B, Kuipers EJ, Kist M, Kusters JG, Bereswill S, van Vliet AH.** 2005. Iron-responsive regulation of the *Helicobacter pylori* iron-cofactored superoxide dismutase SodB is mediated by Fur. J Bacteriol **187**:3687–3692. http://dx.doi.org/10.1128/JB.187.11.3687-3692.2005.

53. **Seyler RW, Jr, Olson JW, Maier RJ.** 2001. Superoxide dismutase-deficient mutants of *Helicobacter pylori* are hypersensitive to oxidative stress and defective in host colonization. Infect Immun **69**:4034–4040. http://dx.doi.org/10.1128/IAI.69.6.4034-4040.2001.

54. **Wang G, Alamuri P, Maier RJ.** 2006. The diverse antioxidant systems of *Helicobacter pylori*. Mol Microbiol **61**:847–860. http://dx.doi.org/10.1111/j.1365-2958.2006.05302.x.

55. **Dian C, Vitale S, Leonard GA, Bahlawane C, Fauquant C, Leduc D, Muller C, de Reuse H, Michaud-Soret I, Terradot L.** 2011. The structure of the *Helicobacter pylori* ferric uptake regulator Fur reveals three functional metal binding sites. Mol Microbiol **79**:1260–1275. http://dx.doi.org/10.1111/j.1365-2958.2010.07517.x.

56. **Gilbreath JJ, Pich OQ, Benoit SL, Besold AN, Cha JH, Maier RJ, Michel SL, Maynard EL, Merrell DS.** 2013. Random and site-specific mutagenesis of the *Helicobacter pylori* ferric uptake regulator provides insight into Fur structure-function relationships. Mol Microbiol **89**:304–323. http://dx.doi.org/10.1111/mmi.12278.

57. **Blanchard TG, Czinn SJ, Correa P, Nakazawa T, Keelan M, Morningstar L, Santana-Cruz I, Maroo A, McCracken C, Shefchek K, Daugherty S, Song Y, Fraser CM, Fricke WF.** 2013. Genome sequences of 65 *Helicobacter pylori* strains isolated from asymptomatic individuals and patients with gastric cancer, peptic ulcer disease, or gastritis. Pathog Dis **68**:39–43. http://dx.doi.org/10.1111/2049-632X.12045.

58. **Miles S, Piazuelo MB, Semino-Mora C, Washington MK, Dubois A, Peek RM, Jr, Correa P, Merrell DS.** 2010. Detailed *in vivo* analysis of the role of *Helicobacter pylori* Fur in colonization and disease. Infect Immun **78**:3073–3082. http://dx.doi.org/10.1128/IAI.00190-10.

59. **den Besten HM, Mols M, Moezelaar R, Zwietering MH, Abee T.** 2009. Phenotypic and transcriptomic analyses of mildly and severely salt-stressed *Bacillus cereus* ATCC 14579 cells. Appl Environ Microbiol **75**:4111–4119. http://dx.doi.org/10.1128/AEM.02891-08.

60. **Höper D, Bernhardt J, Hecker M.** 2006. Salt stress adaptation of *Bacillus subtilis*: a physiological proteomics approach. Proteomics **6**:1550–1562. http://dx.doi.org/10.1002/pmic.200500197.

61. **Hoffmann T, Schutz A, Brosius M, Volker A, Volker U, Bremer E.** 2002. High-salinity-induced iron limitation in *Bacillus subtilis*. J Bacteriol **184**:718–727. http://dx.doi.org/10.1128/JB.184.3.718-727.2002.